Vertical Directional Couplers With Ultra-Short Coupling Length Based on Hybrid Plasmonic Waveguides

Cheng-Han Du and Yih-Peng Chiou, *Member, IEEE*

***Abstract*—we propose and analyze a series of vertical directional couplers based on SOI-compatible hybrid plasmonic waveguides. We investigate two configurations: metal–insulator–metal (MIM) and insulator–metal–insulator (IMI). Both slab and three-dimensional analyses show that MIM directional couplers have better coupling performance such as sub-micron coupling length and lower loss. To ensure the normalized power loss lower than 5%, the coupling length can be chosen as short as 0.492 μm (about one third of the wavelength 1.55 μm). The coupler size can be traded for even lower power loss. In one example, a less-compact design yields 3% power loss, while maintains sub-micron coupling length. We further verified our design with beam propagation analysis. The analysis independently verifies the compact MIM design does show guided mode coupling length along vertical direction can be as short as 0.492 μm.**

***Index Terms*—Hybrid plasmonic waveguides, vertical directional coupler, waveguide mode analysis.**

I. Introduction

OPTICAL circuits have been a promising technology for high-speed signal transferring and processing in recent years. To achieve high-density optical circuits, the miniaturization of optical waveguide dimensions is critical. The size of guided mode field is generally around the operation wavelength in conventional dielectric-based waveguides, such as silicon-on-insulator (SOI) and dielectric slot waveguides. For telecommunication applications, the popular wavelength is 1.55 μm, resulting in overall waveguide dimension in the order of several hundreds of nanometers. This size is relatively larger than modern silicon-based semiconductor devices. In high-density optical circuits, the crosstalk from nearby circuit is also critical. Due to limited field confinement, signals transmitted in dielectric waveguides are susceptible to crosstalk, even with high index-contrast guiding materials. Plasmonic and metal–insulator–metal (MIM) slot waveguides based on surface plasmon polariton (SPP) allow much better confinement. Therefore, they have been proposed as a solution for nanoscale optical circuits [1]–[5]. However, plasmonic waveguides are not good for long-range propagation because metals are very lossy at optical frequency and the field penetrates deeply into the metals in such structures. To compromise the modal size and propagation loss, hybrid plasmonic waveguides (HPWGs) have been proposed [6]. In HPWGs, the guided mode areas of HPGWs are much smaller as compared with dielectric-based waveguides, in order to achieve higher guided field concentration in the gap region between metal and high-index dielectric. The resulting local high field intensity improves signal sensitivity in sensing application [7]. The nanoscale confinement also greatly increases the mode area compactness and reduces the propagation power [6]. In addition, the propagation losses of HPWGs are generally much less than those of plasmonic waveguides, indicating fewer heat dissipation. Overall, HPWGs are attractive for miniaturized optical circuits considering both modal size and propagation loss.

Recently, some researchers in the field of photonic devices also adopt HPWGs for less propagation loss and better miniaturization. Loss compensation using gain media for lossless propagation is reported [8], [9]. Long-range hybrid plasmonic waveguides (LRHPW) are also investigated to further reduce the propagation loss by guided modes of insulator–metal–insulator (IMI) or MIM HPWGs [10]–[14]. The propagation loss of fundamental even mode is much less than that of odd one in a LRHPW. Therefore, optical power is transmitted through fundamental even modes in the waveguides. Applications involving odd guided modes draw little attention due to high propagation loss. Various photonic devices have also been studied to shorten device length for ultra-compact design. Developments of nanoscale lasers have shown great potential of hybrid plasmonic optical devices [15], [16]. Power splitters based on multimode interference (MMI) and Y-branch structures are theoretically analyzed [17]. Microring resonator filters for HPWGs have also been proposed with theoretical analysis and experiment results [18]. Among various photonic devices, directional couplers are a fundamental building block in optical circuits. Several directional couplers based on plasmonic [19] and HPWGs [20]–[22] are studied. Some design schematics are shown in Fig. 1(b) and (c). Even-odd mode beating is the major coupling mechanism of directional couplers. The most straightforward approach to shorten coupling length is to narrow the gap between the two guided regions. If the gap is removed, the wide waveguide becomes a MMI system [23]. In the above

Manuscript received October 17, 2013; revised March 19, 2014; accepted March 25, 2014. Date of publication April 16, 2014; date of current version May 14, 2014. This work was supported in part by the National Science Council of the Taiwan under Grants NSC102-2221-E-002-174 and NSC102-2120-M-110-005, and the Excellent Research Projects of National Taiwan University under Grant 102R89085.

C.-H. Du is with the Graduate Institute of Photonics and Optoelectronics, National Taiwan University, Taipei 10617 Taiwan (e-mail: b2006@csie.ntu.edu.tw).

Y.-P. Chiou is with the Graduate Institute of Photonics and Optoelectronics, the Graduate Institute of Communication Engineering, and the Department of Electrical Engineering, National Taiwan University, Taipei 10617, Taiwan (e-mail: ypchiou@ntu.edu.tw).

Color versions of one or more of the figures in this paper are available online at http://ieeexplore.ieee.org

Digital Object Identifier 10.1109/JLT.2014.2318182

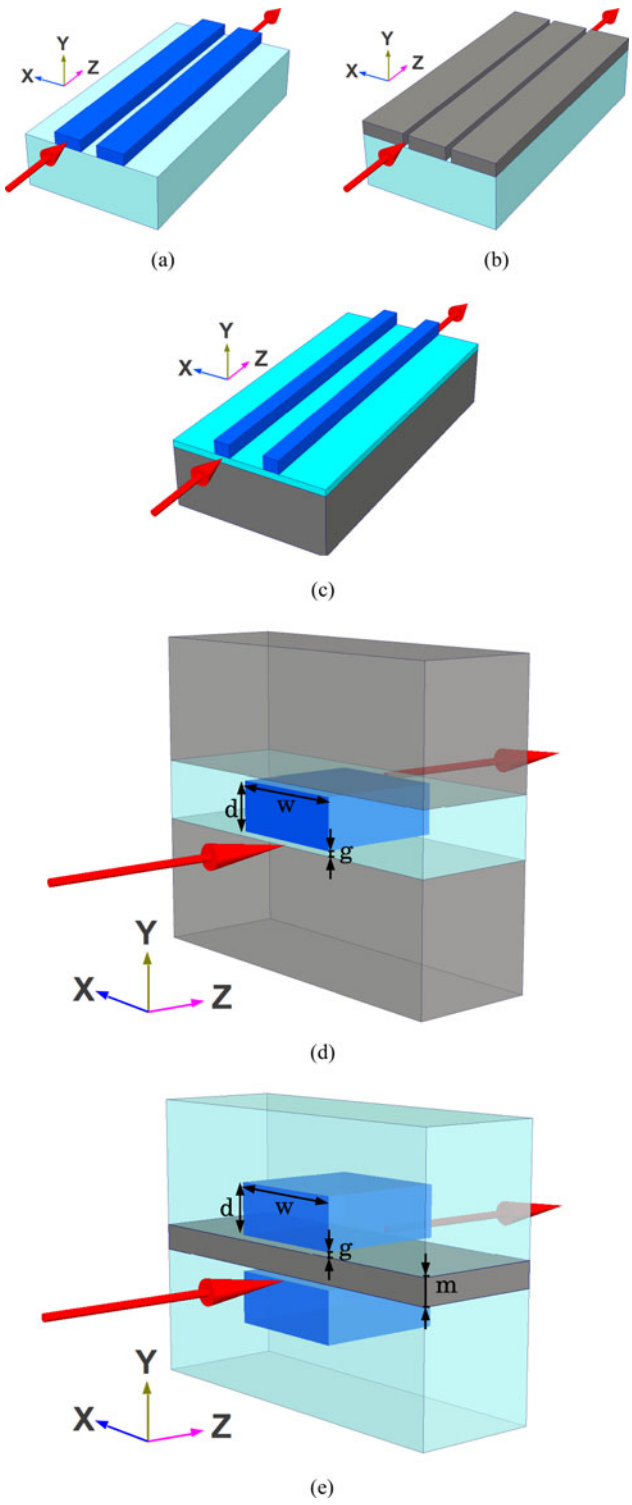

Fig. 1. Schematics of several directional coupler configurations. The gray, darker blue, and light cyan regions are metals, higher permittivity and low-index materials, respectively. Red arrows indicate inputs and outputs of the signals. (a) Dielectric index-guided ridge directional coupler. (b) Plasmonic directional coupler. (c) Lateral hybrid plasmonic directional coupler. (d) Vertical MIM hybrid plasmonic directional coupler. (e) Vertical IMI hybrid plasmonic directional coupler.

mentioned directional couplers, the coupling is often achieved by arranging two identical waveguides along lateral direction. It is in general very difficult to achieve sub-micron coupling length in such arrangement.

In this paper, we propose and analyze an alternative scheme: vertical, instead of lateral, even-odd mode beating, to achieve ultra-compact directional coupling. Several vertical dielectric directional coupler designs were proposed with modulation or amplification capabilities [24], [25], and we apply this design concept to hybrid plasmonic waveguide. We first analyze slab MIM and IMI configurations to obtain the major features of the hybrid plasmonic directional couplers with highly efficient mode solver [26], [27]. The propagation loss of odd modes is critical in our design since it is generally much higher than that of long-range even modes. From the analysis of slab structures, we find that the MIM configuration is a better design since the odd modes work better in terms of power loss. In three-dimensional waveguide mode analysis [28], finite-width directional couplers with the MIM configuration also show superior coupling performance. The sub-micron coupling capability is further modeled and verified by beam propagation analysis. Since the SOI process has been a popular and proven technology in silicon photonics and semiconductor industry, in this paper, we adopt the geometry and material parameters compatible to SOI process. Finally, a conclusion is given.

II. Slab Vertical Hybrid Plasmonic Directional Couplers

We first analyze design feasibility of MIM and IMI configurations as directional couplers. Schematics of both coupler types are illustrated in Fig. 1(d) and (e). Silver, silicon, and silica are selected as device materials in our simulation. They are illustrated by gray, darker blue, and light cyan colors in the figures. Relative permittivities of these materials are $\epsilon_{\mathrm{Ag}} = -129 - j3.3$, $\epsilon_{\mathrm{Si}} = 3.47772^2$, and $\epsilon_{\mathrm{SiO_2}} = 1.5^2$ for telecommunication wavelength 1.55 μm. We investigate propagation characteristics under different silicon height d and silica gap g in both MIM and IMI structures and metal layer thickness m in IMI waveguides. We also investigate the effects of silicon width w in three-dimensional analysis. There are multiple geometry parameters in three-dimensional vertical directional couplers, and simplification is required for efficient performance evaluation. To do the simplification, we first set the range of silicon height d between 200 and 400 nm for SOI-compatible design. Because of small silicon height, a wider silicon block is used for better field confinement. The aspect ratio w/d is larger than or equals to unity, and the major field polarization of guided wave is along y-direction. We then model the simplified MIM and IMI hybrid plasmonic directional couplers with infinite silicon width. The results of the simplified structures show major trends of the waveguide behavior and are very useful for concept explanation and design reference. In addition, with infinite w,

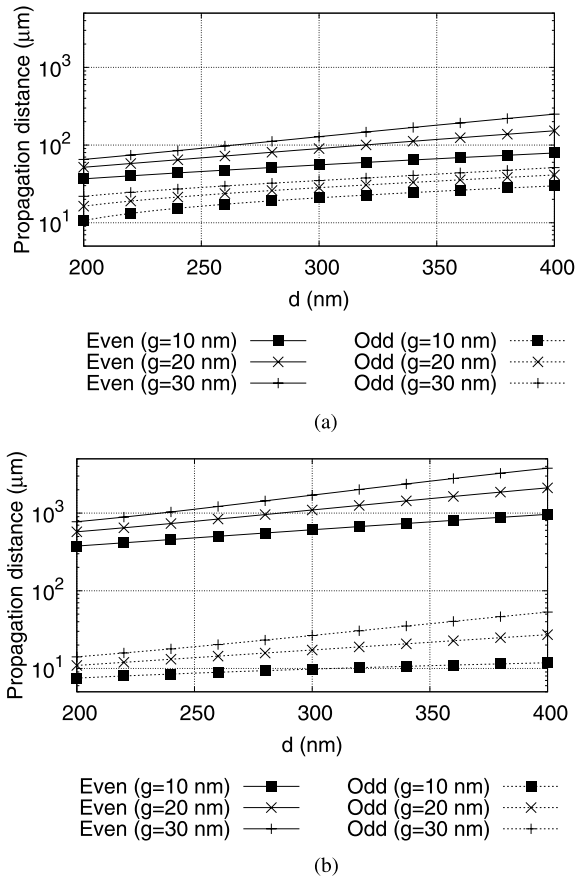

Fig. 2. Propagation distances of even and odd modes with different slab hybrid plasmonic directional coupler configurations. (a) MIM-type. (b) IMI-type with $m = 20$ nm.

the structure can be efficiently modeled with two-dimensional mode solver.

We first calculate the propagation constants β of even and odd guided modes for simplified structures, where the first and the second TM modes are the even and odd modes, respectively. The propagation distance $L_{\rm prop}$ is defined as

$$L_{\rm prop} = \frac{1}{2\Im[\beta]} \tag{1}$$

and the coupling length L_c as

$$L_c = \frac{\pi}{\Re[|\beta_{\rm even} - \beta_{\rm odd}|]}. \tag{2}$$

The $L_{\rm prop}$ is defined as the distance of propagation when mode power decay to e^{-1} of original input power. The propagation distance comparison of MIM and IMI couplers with different geometrical parameters are shown in Fig. 2. The use of narrower gap increases the SPP effects and leads to smaller mode area, but it also increases the propagation loss. In both MIM and IMI waveguides, even modes are much less lossy than odd modes. Referring to Fig. 2(b), the propagation losses of even modes are very low in IMI waveguides with very thin metal layer. This feature is very useful for long-range propagation design. Meanwhile, the losses of odd modes are extremely high because of deeper field penetration into the metal layer [10]. When the metal layer of IMI waveguide is thicker, e.g., $m = 80$ nm, the upper and lower waveguides are nearly decoupled and the field penetration into the metal layer for odd modes is decreased. These results match with earlier theoretical reports [10]. On the other hand, in MIM HPWGs, the loss difference of even and odd modes are relatively smaller than that in IMI waveguides with $m = 20$ nm. The more balanced loss figure in MIM structures is because of the guiding provided by silicon and dual metal layers. The guiding mechanism yields more field penetration in dielectric materials and avoids strong field penetration in the metal layer for odd modes. In comparison, the silicon layer in the IMI structure with very thin metal layer does not provide sufficient guiding because of the domination of the SPP effect. Note that for the worst case of odd mode in MIM waveguide, its propagation distance is approximately 10.7 μm. Since it is several times larger than the coupling length, the waveguides are good for directional coupler applications.

To further analyze the coupling characteristics of slab hybrid plasmonic directional couplers, we introduce the ratio R, defined as

$$R = \frac{L_{\rm prop}({\rm odd})}{L_c}. \tag{3}$$

This ratio can be regarded as a benchmark of coupler performance and efficiency after a coupling length. The choice of odd mode in the ratio is because the higher loss of odd mode is the major source of performance degradation. Both results of coupling length and ratio R are shown in Fig. 3. The normalized odd mode power loss $f_{\rm odd}$ in the figure is defined as

$$f_{\rm odd} = 1 - e^{-1/R}, \tag{4}$$

which indicates odd mode power loss after one coupling process. The R values are approximately larger than 9.49, 19.50, or 32.83 for normalized odd mode power loss of 10%, 5%, or 3%, respectively. The threshold R values for of 10%, 5%, or 3% are illustrated as magenta, red, and brown lines in all R ratio comparison figures. From Fig. 3(a), we find that sub-micron coupling length can be easily achieved in MIM waveguides with d less than 300 nm. When the most compact setting of $(d, g) = (200, 10)$ nm is used, the coupling length can be as low as 0.47 μm, while the corresponding R value is still larger than 22. For $f_{\rm odd}$ lower than 5%, the resulting MIM waveguide shows great potential as a high-performance and ultra-compact directional coupler. If the gap size is set to 30 nm and d remains the same, the R value and $f_{\rm odd}$ can be further improved with slightly longer coupling length. The R value can be larger than 34 with $f_{\rm odd}$ lower than 3%, while L_c is approximately 0.64 μm, which is still sub-micron. This choice of parameters allows better power conservation while maintains compactness.

The results of IMI directional couplers are shown in Fig. 3(b). With $m = 20$ nm, the coupling lengths are in the wavelength-scale. Combined with higher propagation losses of odd modes, the resulting R values at $g = 10$ nm are less than 5. This indicates that more than 18% of odd mode power is lost after one coupling process. Increasing m to 80 nm, we find the minimum coupling distance is over

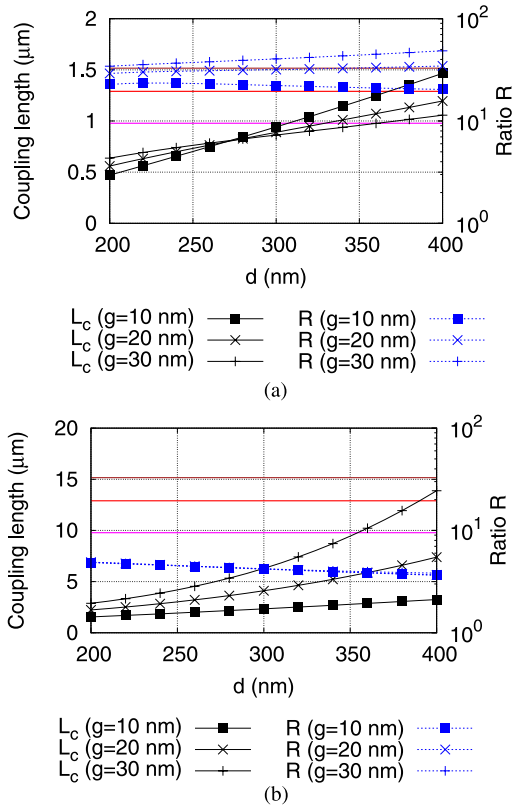

Fig. 3. Coupling length and ratio R comparison of different slab hybrid plasmonic waveguide configurations. The magenta, red, and brown lines illustrate the normalized odd mode power losses of 10%, 5%, and 3%, respectively. (a) MIM-type. (b) IMI-type with $m = 20$ nm.

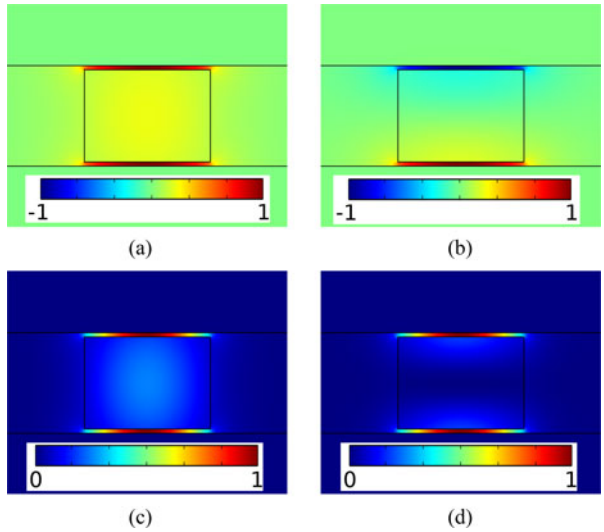

Fig. 4. E_y field and power flow distributions of even and odd modes in a MIM-type finite-width hybrid plasmonic waveguide. The geometry parameters in this case are $(w, d, g) = (300, 220, 10)$ nm. Units of all color bars are arbitrary unit. (a) Even mode, E_y field. (b) Odd mode, E_y field. (c) Even mode, Poynting flux. (d) Odd mode, Poynting flux.

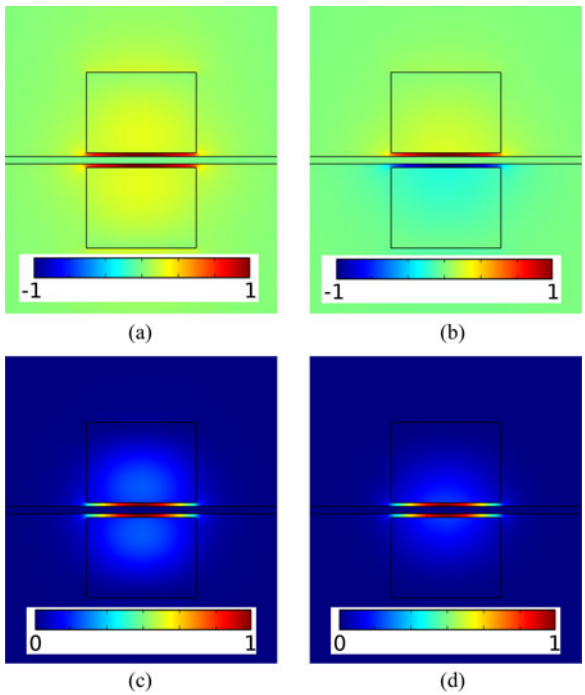

Fig. 5. E_y field and power flow distributions of even and odd modes in a IMI-type finite-width hybrid plasmonic waveguide. The geometry parameters in this case are $(w, d, g, m) = (300, 220, 10, 20)$ nm. Units of all color bars are arbitrary unit. (a) Even mode, E_y field. (b) Odd mode, E_y field. (c) Even mode, Poynting flux. (d) Odd mode, Poynting flux.

30 μm. The corresponding R value is less than unity, and f_{odd} is higher than 63%. As explained earlier, the upper and lower waveguides are almost decoupled when $m = 80$ nm, and this makes directional coupling in IMI structure with a thick metal layer ineffective.

III. Three-Dimensional Vertical Hybrid Plasmonic Directional Couplers with Finite-Width Silicon

For practical design, we consider the finite-width silicon in the directional coupler design with schematics illustrated in Fig. 1(d) and (e). Because the slab waveguide analysis in Section II shows that sub-micron coupling can be achieved with d less than 300 nm, we limit the simulation range of d up to 300 nm. Section II also shows the coupling in IMI structure with thick metal layer is not good. Therefore, we will consider MIM and only IMI couplers with $m = 20$ nm in this section. Due to the narrow height of the waveguide, we choose wide silicon core to provide sufficient horizontal confinement. The finite silicon width w is set to 300, 400, and 500 nm for comparison. As shown in Section II, odd modes have higher propagation loss than even ones. The performance of HPWG directional couplers will mainly depend on their odd modes. Therefore, we will focus and demonstrate more on simulation results of odd mode in this section. Referring to Figs. 4 and 5, the Poynting flux S_z and E_y field components of both even and odd modes of finite-width waveguide are shown. The results verify high field concentration in the gap regions and small guiding area, which we have mentioned previously.

As shown in Fig. 6(a), if thicker silicon or wider gap is used in MIM coupler, odd mode guiding behavior is less dependent

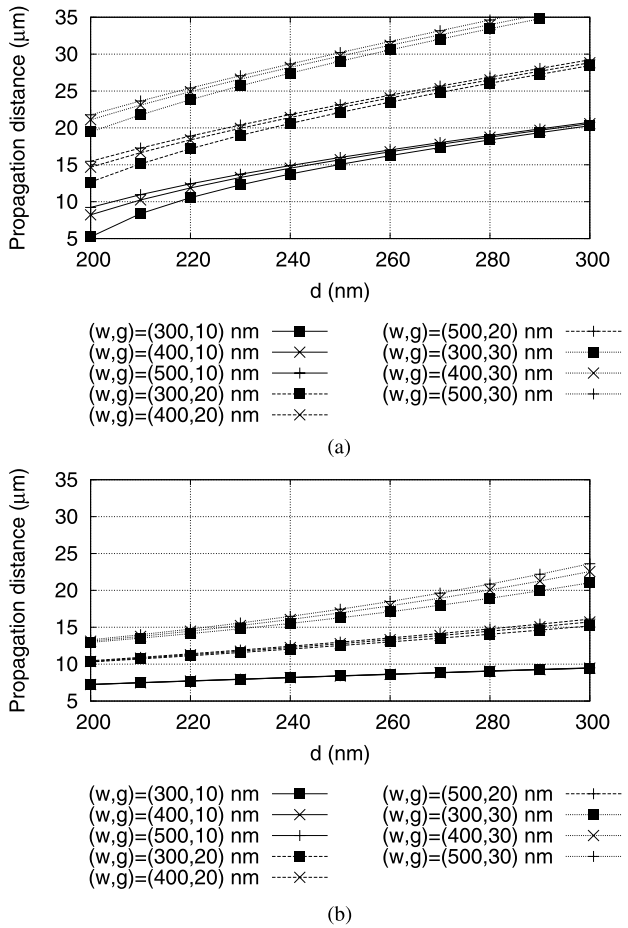

Fig. 6. Propagation distance comparison of odd mode in finite-width hybrid plasmonic waveguide. (a) MIM-type. (b) IMI-type with $m = 20$ nm.

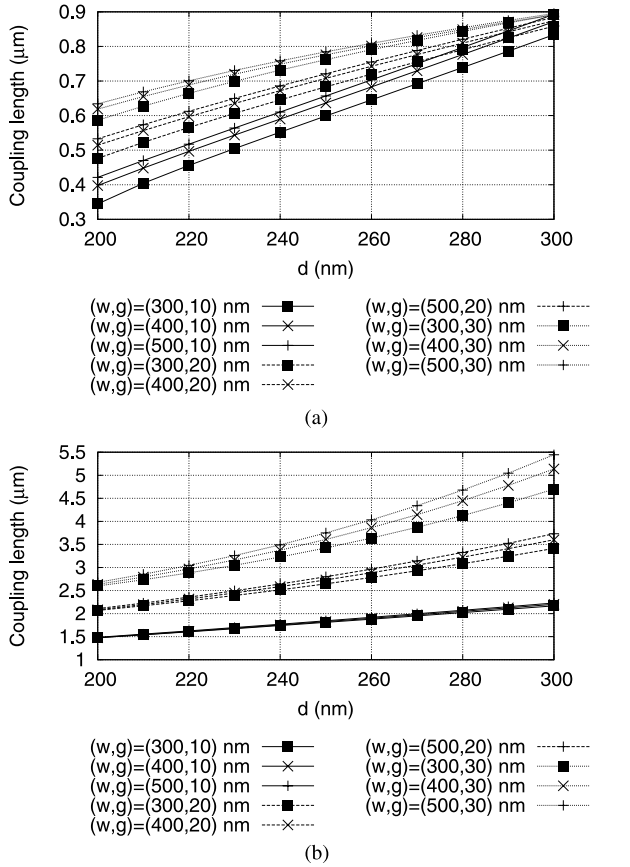

Fig. 7. Coupling length comparison of finite-width hybrid plasmonic waveguide. (a) MIM-type. (b) IMI-type with $m = 20$ nm.

on silicon width w. Waveguides with narrower width w will not result in significant loss. With $g = 10$ nm and $w = 300$ nm, the decrease of the propagation distance becomes significant for $d < 240$ nm. From Fig. 6(b), we find propagation loss is dominated by gap size, as thin metal layer thickness of IMI coupler is fixed. Overall, both finite-width MIM and IMI HPWGs show only moderate increases of propagation loss compared with their corresponding slab cases.

We also show the comparison of coupling length in Fig. 7(a) and (b). The coupling length L_c of MIM couplers are less than 1 μm for all parameter combinations investigated. L_c can be less than 0.5 μm with gap sizes of 10 nm and d equal to or less than 220 nm, which are very compact. The coupling lengths of the compact structures with finite silicon width are even shorter than slab MIM waveguides, as $L_c < 0.5$ μm. The coupling lengths of IMI couplers are longer than those of MIM couplers, while the propagation distances of the former are shorter than those of the latter. Simulation shows that the differences of coupling lengths between finite- and infinite-width IMI HPWGs are less than 10% when gap size g is 10 nm.

Again, we introduce ratio R to benchmark their performance. The R value comparison is shown in Fig. 8(a) and (b). All cases of MIM couplers show $R > 20$ except for $(w, d, g) = (300, 200, 10)$ nm, while the R values of all IMI couplers are less than 5. This means finite-width silicon MIM hybrid plasmonic directional couplers also provide ultra-compactness and high coupling efficiency. Combined with coupling length results, we have several highly-compact design choices. For example, the coupling length is shorter than 0.5 μm when $(w, d, g) = (300, 220, 10)$ nm. Normalized odd mode loss $f_{\rm odd}$ is lower than 5% after coupling at the same time. If larger gap $g = 30$ nm is used, the R values are significantly higher and $f_{\rm odd}$'s are less than 3% ratio for all geometry settings.

From the modal analysis, we find that MIM HPWG is ideal for high-performance directional couplers. We further use full-vectorial beam propagation method (BPM) [29] to simulate the ultra-compact MIM directional couplers. The BPM gives the field distribution from one-way propagation based on slow-varying envelope approximation. The formulation is described as $k_0 n_0 \psi \gg |\partial\psi/\partial z|$, where ψ is wave envelope with fast phase-varying term $e^{-jk_0 n_0 z}$ extracted and n_0 is a reference effective index. The BPM in our simulation is based on magnetic field formulation to avoid field singularity near silicon corner. Since the dominant components of quasi-TM guided wave are E_y and H_x fields, the Poynting flux S_z can be approximated as

$$S_z = \frac{1}{2}\Re[(\mathbf{E}^* \times \mathbf{H}) \cdot \hat{z}] \approx -\frac{1}{2}E_y^* H_x, \tag{5}$$

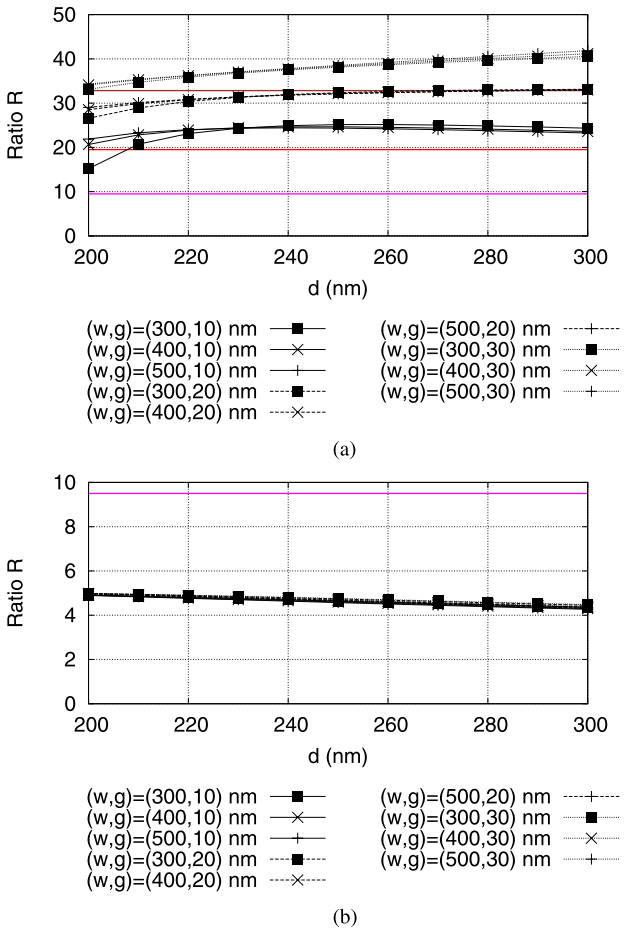

Fig. 8. Ratio R comparison of finite-width hybrid plasmonic waveguide. (a) MIM-type. (b) IMI-type with $m = 20$ nm.

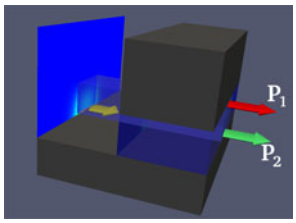

Fig. 9. Schematic of beam propagation analysis for vertical directional coupler based on HPWGs.

where E_y and H_x are wave envelopes without phase term $e^{-jk_0 n_0 z}$. With slow-varying envelope approximation [30], the relation of approximated Poynting flux flow S_z and H_x can be expressed as

$$S_z \underset{\sim}{\propto} \frac{|H_x|^2}{\epsilon}. \tag{6}$$

In the BPM simulation, the silicon width, height, and guiding gap sizes (w, d, g) of the hybrid plasmonic directional coupler are $(300, 220, 10)$ nm. From the simulation schematic in Fig. 9, the single-slot guided mode is launched into the lower gap. The approximated mode power distribution of the launched guided

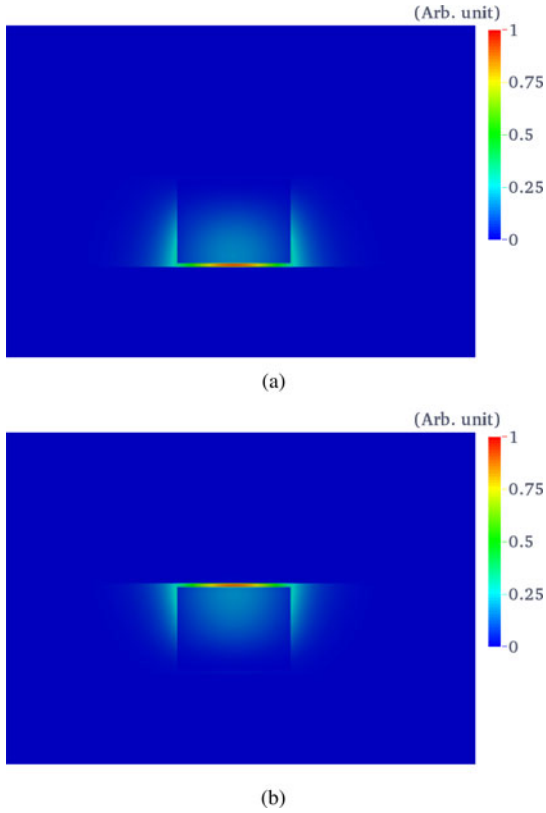

Fig. 10. Approximated power flow of MIM-type vertical hybrid plasmonic directional coupler. (a) $z = 0.0$ μm. (b) $z = 0.492\mu$m.

wave is shown in Fig. 10(a). We investigate the crosstalk by defining the figure of merit (FoM) as

$$\text{FoM} = 10\log\frac{P_1}{P_2} = 10\log\left(\frac{\int_{\text{Upper gap}} S_z dxdy}{\int_{\text{Lower gap}} S_z dxdy}\right) \tag{7}$$

where the gap cross-section is $w \times g$ as illustrated in Fig. 1(d).

From earlier modal analysis of even and odd modes, L_c for $(w, d, g) = (300, 220, 10)$ nm is about 0.456 μm. From BPM calculation, the approximated power distribution at $z = 0.492$ μm as shown in Fig. 10(b), shows that the coupled mode power ratio is approximately 99%. This indicates highly efficient mode coupling between vertical directional coupler and input/output waveguides. In the crosstalk calculation, the FoM at $z = 0.492$ μm is approximately 17.6 dB. With low propagation losses and short coupling lengths, the proposed design can achieve very high coupling efficiency, verified by both modal analysis and beam propagation analysis.

IV. Conclusion

We propose an alternative design of vertically stacked directional couplers based on SOI-compatible ultra-compact HPWGs. Symmetric MIM and IMI slab HPWGs are considered. From the slab waveguide analysis, it is shown that MIM directional couplers can achieve both sub-micron coupling and high coupling efficiency. It is also shown that MIM waveguides have better performance in terms of the coupling length and

propagation loss of the fundamental odd mode than IMI waveguides. We also simulate practical MIM and IMI directional couplers with finite-width. The results show sub-micron coupling length in most finite-width MIM directional couplers. For some highly compact MIM coupler designs, the coupling length can be even shorter than 0.5 μm while the propagation loss during coupling is kept lower than 5%. We further verify the details of the coupling mechanism by the beam propagation analysis. With the high efficiency of power transfer and sub-micron coupling length, our proposed vertical MIM directional couplers will be very useful in high-density optical circuits.

ACKNOWLEDGEMENTS

The authors gratefully acknowledge the help of Dr. M.-C. Ho, whose suggestion to their research has made the product of this manuscript much better.

REFERENCES

[1] W. L. Barnes, A. Dereux, and T. W. Ebbesen, "Surface plasmon subwavelength optics," *Nature*, vol. 424, pp. 824–830, 2003.
[2] R. Charbonneau, N. Lahoud, G. Mattiussi, and P. Berini, "Demonstration of integrated optics elements based on long-ranging surface plasmon polaritons," *Opt. Exp.*, vol. 13, pp. 977–984, 2005.
[3] L. Liu, Z. Han, and S. He, "Novel surface plasmon waveguide for high integration," *Opt. Exp.*, vol. 13, pp. 6645–6650, 2005.
[4] J. A. Dionne, L. A. Sweatlock, H. A. Atwater, and A. Polman, "Plasmon slot waveguides: Towards chip-scale propagation with subwavelength-scale localization, " *Phys. Rev. B*, vol. 73, p. 035407, 2006.
[5] G. Veronis and S. Fan, "Modes of subwavelength plasmonic slot waveguides," *J. Lightw. Technol.*, vol. 25, no. 9, pp. 2511–2521, Sep. 2007.
[6] R. F. Oulton, V. J. Sorger, D. A. Genov, D. F. P. Pile, and X. Zhang, "A hybrid plasmonic waveguide for subwavelength confinement and long-range propagation," *Nature Photon.*, vol. 2, no. 8, pp. 496–500, 2008.
[7] L. Zhou, X. Sun, X. Li, and J. Chen, "Miniature microring resonator sensor based on a hybrid plasmonic waveguide," *Sensors*, vol. 11, pp. 6856–6867, 2011.
[8] J. Zhang, L. Cai, W. Bai, Y. Xu, and G. Song, "Hybrid plasmonic waveguide with gain medium for lossless propagation with nanoscale confinement," *Opt. Lett.*, vol. 36, no. 12, pp. 2312–2314, 2011.
[9] D. Dai, Y. Shi, S. He, L. Wosinski, and L. Thylen, "Gain enhancement in a hybrid plasmonic nano-waveguide with a low-index or high-index gain medium," *Opt. Exp.*, vol. 19, pp. 12925–12936, 2011.
[10] P. Berini, "Long-range surface plasmon polaritons," *Adv. Opt. Photon.*, vol. 1, no. 3, pp. 484–588, 2009.
[11] Y. Bian, Z. Zheng, X. Zhao, J. Zhu, and T. Zhou, "Symmetric hybrid surface plasmon polariton waveguides for 3D photonic integration," *Opt. Exp.*, vol. 17, no. 23, pp. 21320–21325, 2009.
[12] L. Chen, T. Zhang, X. Li, and W. Huang, "Novel hybrid plasmonic waveguide consisting of two identical dielectric nanowires symmetrically placed on each side of a thin metal film," *Opt. Exp.*, vol. 20, no. 18, pp. 20535–20544, 2012.
[13] C. Xiang and J. Wang, "Long-range hybrid plasmonic slot waveguide," *IEEE Photon. J.*, vol. 5, no. 2, p. 4800311, Apr.2013.
[14] Y. Bian and Q. Gong, "Optical performance of one-dimensional hybrid metal-insulator-metal structures at telecom wavelength," *Opt. Commun.*, vol. 308, pp. 30–35, 2013.
[15] R. F. Oulton, V. J. Sorger, T. Zentgraf, R.-M. Ma, C. Gladden, L. Dai, G. Bartel, and X. Zhang, "Plasmon lasers at deep subwavelength scale," *Nature*, vol. 461, pp. 629–632, 2009.
[16] Y.-J. Lu, J. Kim, H.-Y. Chen, C. Wu, N. Dabidian, C. E. Sanders, C.-Y. Wang, M.-Y. Lu, B.-H. Li, X. Qiu, W.-H. Chang, L.-J. Chen, G. Shvets, C.-K. Shih, and S. Gwo, "Plasmonic nanolaser using epitaxially grown silver film," *Science*, vol. 337, no. 6093, pp. 450–453, 2012.
[17] J. Wang, X. Guan, Y. He, Y. Shi, Z. Wang, S. He, P. Holmström, L. Wosinski, L. Thylen, and D. Dai, "Sub-μm^2 power splitters by using silicon hybrid plasmonic waveguides," *Opt. Exp.*, vol. 19, pp. 838–847, 2011.
[18] H.-S. Chu, Y. Akimov, P. Bai, and E.-P. Li, "Submicrometer radius and highly confined plasmonic ring resonator filters based on hybrid metal-oxide-semiconductor waveguide," *Opt. Lett.*, vol. 37, no. 21, pp. 4564–4566, 2012.
[19] D. K. Gramotnev, K. C. Vernon, and D. F. P. Pile, "Directional coupler using gap plasmon waveguides," *Appl. Phys. B*, vol. 93, no. 1, pp. 99–106, 2008.
[20] M. Z. Alam, J. Niklas Caspers, J. S. Aitchison, and M. Mojahedi, "Compact low loss and broadband hybrid plasmonic directional coupler," *Opt. Exp.*, vol. 21, no. 13, pp. 16029–16034, 2013.
[21] Q. Li, Y. Song, G. Zhou, Y. Su, and M. Qiu, "Asymmetric plasmonic-dielectric coupler with short coupling length, high extinction ratio, and low insertion loss," *Opt. Lett.*, vol. 35, no. 19, pp. 3153–3155, 2010.
[22] F. Lou, Z. Wang, D. Dai, L. Thylen, and L. Wosinski, "Experimental demonstration of ultra-compact directional couplers based on silicon hybrid plasmonic waveguides," *Appl. Phys. Lett.*, vol. 100, no. 24, p. 241105, 2012.
[23] Z. Zhu, C. E. Garcia-Ortiz, Z. Han, I. P. Radko, and S. I. Bozhevolnyi, "Compact and broadband directional coupling and demultiplexing in dielectric-loaded surface plasmon polariton waveguides based on the multimode interference effect," *Appl. Phys. Lett.*, vol. 103, no. 6, p. 061108, 2013.
[24] V. Lemoine, M. Papuchon, J. P. Pocholle, P. Le Barney, and P. Robin, "Electro-optic modulator and second-harmonic generator with nonlinear polymers," *Synth. Met.*, vol. 54, pp. 147–153, 1993.
[25] G. Glastre, D. Rondi, A. Enard, E. Lallier, R. Blondeau, and M. Papuchon, "Monolithic integration of 2×2 switch and optical amplifier with 0dB fibre to fibre insertion loss grown by LP-MOCVD," *Electron. Lett.*, vol. 29, no. 1, pp. 124–126, 1993.
[26] Y.-P. Chiou, and C.-H. Du, "Arbitrary-order interface conditions for slab structures and their applications in waveguide analysis, " *Opt. Exp.*, vol. 18, no. 5, pp. 4088–4102, 2010.
[27] M. T. Noghani, and M. H. V. Samiei, "Analysis and optimum design of hybrid plasmonic slab waveguides," *Plasmonics*, vol. 8, no. 2, pp. 1155–1168, 2013.
[28] Y.-P. Chiou, and C.-H. Du, "Arbitrary-order full-vectorial interface conditions and higher-order finite-difference analysis of optical waveguides," *J. Lightw. Technol.*, vol. 29, no. 22, pp. 3445–3452, Nov. 2011.
[29] C.-H. Du, and Y.-P. Chiou, "Beam propagation analysis using higher-order full-vectorial finite-difference method," *Opt., Quantum Eletron.*, vol. 45, no. 7, pp. 769–774, 2013.
[30] J. Yamauchi, M. Koshihara, and H. Nakano, "Numerical analysis of a waveguide-based demultiplexer with two multilayer filters," *IEEE Photon. Technol. Lett.*, vol. 17, no. 2, pp. 366–368, Feb. 2005.

Cheng-Han Du was born in Taipei, Taiwan, in December 1984. He received the B.S. degree from the Department of Computer Science and Information Engineering, and the M.S. and Ph.D. degrees from the Graduate Institute of Photonics and Optoelectronics, National Taiwan University, Taipei, in 2007, 2009, and 2014, respectively. He is currently a Postdoctoral Research Fellow in the Department of Mathematics, National Taiwan University. His research interests include numerical method development for waveguide modeling, photonic device design, and high-performance computing.

Yih-Peng Chiou (M'03) was born in Taoyuan, Taiwan, in 1969. He received the B.S. and Ph.D. degrees in electrical engineering from National Taiwan University, Taipei, Taiwan, in 1992 and 1998, respectively. From 1999 to 2000, he was with Taiwan Semiconductor Manufacturing Company, where he was involved in plasma enhanced chemical vapor deposition of dielectric films. From 2001 to 2003, he was with RSoft Design Group, New York, where he was involved in the modeling of simulation techniques and developing of photonic computer-aided design (CAD) tools. Since 2003, he has been with the Faculty of the Graduate Institute of Electro-Optical Engineering and Department of Electrical Engineering, National Taiwan University. His current research interests include modeling and CAD of optoelectronics, which includes photonic crystals, nanostructures, waveguide devices, optical fiber devices, light extraction enhancement in LED, display, solar cell devices, and the development and improvement of numerical techniques in optoelectronics.